Measurement of the Branching Fraction and *CP* Content for the Decay $B^0 \to D^{*+}D^{*-}$

B. Aubert,[1] D. Boutigny,[1] J.-M. Gaillard,[1] A. Hicheur,[1] Y. Karyotakis,[1] J. P. Lees,[1] P. Robbe,[1] V. Tisserand,[1]
A. Zghiche,[1] A. Palano,[2] A. Pompili,[2] G. P. Chen,[3] J. C. Chen,[3] N. D. Qi,[3] G. Rong,[3] P. Wang,[3] Y. S. Zhu,[3]
G. Eigen,[4] B. Stugu,[4] G. S. Abrams,[5] A. W. Borgland,[5] A. B. Breon,[5] D. N. Brown,[5] J. Button-Shafer,[5]
R. N. Cahn,[5] M. S. Gill,[5] A. V. Gritsan,[5] Y. Groysman,[5] R. G. Jacobsen,[5] R. W. Kadel,[5] J. Kadyk,[5] L. T. Kerth,[5]
Yu. G. Kolomensky,[5] J. F. Kral,[5] C. LeClerc,[5] M. E. Levi,[5] G. Lynch,[5] P. J. Oddone,[5] M. Pripstein,[5] N. A. Roe,[5]
A. Romosan,[5] M. T. Ronan,[5] V. G. Shelkov,[5] A. V. Telnov,[5] W. A. Wenzel,[5] T. J. Harrison,[6] C. M. Hawkes,[6]
D. J. Knowles,[6] S. W. O'Neale,[6] R. C. Penny,[6] A. T. Watson,[6] N. K. Watson,[6] T. Deppermann,[7] K. Goetzen,[7]
H. Koch,[7] M. Kunze,[7] B. Lewandowski,[7] K. Peters,[7] H. Schmuecker,[7] M. Steinke,[7] N. R. Barlow,[8] W. Bhimji,[8]
N. Chevalier,[8] P. J. Clark,[8] W. N. Cottingham,[8] B. Foster,[8] C. Mackay,[8] F. F. Wilson,[8] K. Abe,[9] C. Hearty,[9]
T. S. Mattison,[9] J. A. McKenna,[9] D. Thiessen,[9] S. Jolly,[10] A. K. McKemey,[10] V. E. Blinov,[11] A. D. Bukin,[11]
D. A. Bukin,[11] A. R. Buzykaev,[11] V. B. Golubev,[11] V. N. Ivanchenko,[11] A. A. Korol,[11] E. A. Kravchenko,[11]
A. P. Onuchin,[11] S. I. Serednyakov,[11] Yu. I. Skovpen,[11] V. I. Telnov,[11] A. N. Yushkov,[11] D. Best,[12] M. Chao,[12]
D. Kirkby,[12] A. J. Lankford,[12] M. Mandelkern,[12] S. McMahon,[12] D. P. Stoker,[12] K. Arisaka,[13] C. Buchanan,[13]
S. Chun,[13] D. B. MacFarlane,[14] S. Prell,[14] Sh. Rahatlou,[14] G. Raven,[14] V. Sharma,[14] C. Campagnari,[15]
B. Dahmes,[15] P. A. Hart,[15] N. Kuznetsova,[15] S. L. Levy,[15] O. Long,[15] A. Lu,[15] M. A. Mazur,[15] J. D. Richman,[15]
W. Verkerke,[15] J. Beringer,[16] A. M. Eisner,[16] M. Grothe,[16] C. A. Heusch,[16] W. S. Lockman,[16] T. Pulliam,[16]
T. Schalk,[16] R. E. Schmitz,[16] B. A. Schumm,[16] A. Seiden,[16] M. Turri,[16] W. Walkowiak,[16] D. C. Williams,[16]
M. G. Wilson,[16] E. Chen,[17] G. P. Dubois-Felsmann,[17] A. Dvoretskii,[17] D. G. Hitlin,[17] S. Metzler,[17]
J. Oyang,[17] F. C. Porter,[17] A. Ryd,[17] A. Samuel,[17] S. Yang,[17] R. Y. Zhu,[17] S. Devmal,[18] S. Jayatilleke,[18]
G. Mancinelli,[18] B. T. Meadows,[18] M. D. Sokoloff,[18] T. Barillari,[19] P. Bloom,[19] W. T. Ford,[19] U. Nauenberg,[19]
A. Olivas,[19] P. Rankin,[19] J. Roy,[19] J. G. Smith,[19] W. C. van Hoek,[19] L. Zhang,[19] J. Blouw,[20] J. L. Harton,[20]
M. Krishnamurthy,[20] A. Soffer,[20] W. H. Toki,[20] R. J. Wilson,[20] J. Zhang,[20] T. Brandt,[21] J. Brose,[21] T. Colberg,[21]
M. Dickopp,[21] R. S. Dubitzky,[21] A. Hauke,[21] E. Maly,[21] R. Müller-Pfefferkorn,[21] S. Otto,[21] K. R. Schubert,[21]
R. Schwierz,[21] B. Spaan,[21] L. Wilden,[21] D. Bernard,[22] G. R. Bonneaud,[22] F. Brochard,[22] J. Cohen-Tanugi,[22]
S. Ferrag,[22] S. T'Jampens,[22] Ch. Thiebaux,[22] G. Vasileiadis,[22] M. Verderi,[22] A. Anjomshoaa,[23] R. Bernet,[23]
A. Khan,[23] D. Lavin,[23] F. Muheim,[23] S. Playfer,[23] J. E. Swain,[23] J. Tinslay,[23] M. Falbo,[24] C. Borean,[25] C. Bozzi,[25]
L. Piemontese,[25] E. Treadwell,[26] F. Anulli,[27, *] R. Baldini-Ferroli,[27] A. Calcaterra,[27] R. de Sangro,[27] D. Falciai,[27]
G. Finocchiaro,[27] P. Patteri,[27] I. M. Peruzzi,[27, *] M. Piccolo,[27] Y. Xie,[27] A. Zallo,[27] S. Bagnasco,[28] A. Buzzo,[28]
R. Contri,[28] G. Crosetti,[28] M. Lo Vetere,[28] M. Macri,[28] M. R. Monge,[28] S. Passaggio,[28] F. C. Pastore,[28]
C. Patrignani,[28] E. Robutti,[28] A. Santroni,[28] S. Tosi,[28] M. Morii,[29] R. Bartoldus,[30] R. Hamilton,[30] U. Mallik,[30]
J. Cochran,[31] H. B. Crawley,[31] P.-A. Fischer,[31] J. Lamsa,[31] W. T. Meyer,[31] E. I. Rosenberg,[31] J. YI,[31]
G. Grosdidier,[32] A. Höcker,[32] H. M. Lacker,[32] S. Laplace,[32] F. Le Diberder,[32] V. Lepeltier,[32] A. M. Lutz,[32]
S. Plaszczynski,[32] M. H. Schune,[32] S. Trincaz-Duvoid,[32] G. Wormser,[32] R. M. Bionta,[33] V. Brigljević,[33]
D. J. Lange,[33] M. Mugge,[33] K. van Bibber,[33] D. M. Wright,[33] A. J. Bevan,[34] J. R. Fry,[34] E. Gabathuler,[34]
R. Gamet,[34] M. George,[34] M. Kay,[34] D. J. Payne,[34] R. J. Sloane,[34] C. Touramanis,[34] M. L. Aspinwall,[35]
D. A. Bowerman,[35] P. D. Dauncey,[35] U. Egede,[35] I. Eschrich,[35] G. W. Morton,[35] J. A. Nash,[35] P. Sanders,[35]
D. Smith,[35] J. J. Back,[36] G. Bellodi,[36] P. Dixon,[36] P. F. Harrison,[36] R. J. L. Potter,[36] H. W. Shorthouse,[36]
P. Strother,[36] P. B. Vidal,[36] G. Cowan,[37] S. George,[37] M. G. Green,[37] A. Kurup,[37] C. E. Marker,[37]
T. R. McMahon,[37] S. Ricciardi,[37] F. Salvatore,[37] G. Vaitsas,[37] D. Brown,[38] C. L. Davis,[38] J. Allison,[39]
R. J. Barlow,[39] J. T. Boyd,[39] A. C. Forti,[39] F. Jackson,[39] G. D. Lafferty,[39] N. Savvas,[39] J. H. Weatherall,[39]
J. C. Williams,[39] A. Farbin,[40] A. Jawahery,[40] V. Lillard,[40] J. Olsen,[40] D. A. Roberts,[40] J. R. Schieck,[40]
G. Blaylock,[41] C. Dallapiccola,[41] K. T. Flood,[41] S. S. Hertzbach,[41] R. Kofler,[41] V. B. Koptchev,[41] T. B. Moore,[41]
H. Staengle,[41] S. Willocq,[41] B. Brau,[42] R. Cowan,[42] G. Sciolla,[42] F. Taylor,[42] R. K. Yamamoto,[42] M. Milek,[43]
P. M. Patel,[43] F. Palombo,[44] J. M. Bauer,[45] L. Cremaldi,[45] V. Eschenburg,[45] R. Kroeger,[45] J. Reidy,[45]
D. A. Sanders,[45] D. J. Summers,[45] C. Hast,[46] J. Y. Nief,[46] P. Taras,[46] H. Nicholson,[47] C. Cartaro,[48] N. Cavallo,[48, †]
G. De Nardo,[48] F. Fabozzi,[48] C. Gatto,[48] L. Lista,[48] P. Paolucci,[48] D. Piccolo,[48] C. Sciacca,[48] J. M. LoSecco,[49]

J. R. G. Alsmiller,[50] T. A. Gabriel,[50] J. Brau,[51] R. Frey,[51] E. Grauges,[51] M. Iwasaki,[51] N. B. Sinev,[51] D. Strom,[51] F. Colecchia,[52] F. Dal Corso,[52] A. Dorigo,[52] F. Galeazzi,[52] M. Margoni,[52] G. Michelon,[52] M. Morandin,[52] M. Posocco,[52] M. Rotondo,[52] F. Simonetto,[52] R. Stroili,[52] E. Torassa,[52] C. Voci,[52] M. Benayoun,[53] H. Briand,[53] J. Chauveau,[53] P. David,[53] Ch. de la Vaissière,[53] L. Del Buono,[53] O. Hamon,[53] Ph. Leruste,[53] J. Ocariz,[53] M. Pivk,[53] L. Roos,[53] J. Stark,[53] P. F. Manfredi,[54] V. Re,[54] V. Speziali,[54] E. D. Frank,[55] L. Gladney,[55] Q. H. Guo,[55] J. Panetta,[55] C. Angelini,[56] G. Batignani,[56] S. Bettarini,[56] M. Bondioli,[56] F. Bucci,[56] E. Campagna,[56] M. Carpinelli,[56] F. Forti,[56] M. A. Giorgi,[56] A. Lusiani,[56] G. Marchiori,[56] F. Martinez-Vidal,[56] M. Morganti,[56] N. Neri,[56] E. Paoloni,[56] M. Rama,[56] G. Rizzo,[56] F. Sandrelli,[56] G. Simi,[56] G. Triggiani,[56] J. Walsh,[56] M. Haire,[57] D. Judd,[57] K. Paick,[57] L. Turnbull,[57] D. E. Wagoner,[57] J. Albert,[58] C. Lu,[58] V. Miftakov,[58] S. F. Schaffner,[58] A. J. S. Smith,[58] A. Tumanov,[58] E. W. Varnes,[58] G. Cavoto,[59] D. del Re,[59] R. Faccini,[14,59] F. Ferrarotto,[59] F. Ferroni,[59] M. A. Mazzoni,[59] S. Morganti,[59] G. Piredda,[59] M. Serra,[59] C. Voena,[59] S. Christ,[60] R. Waldi,[60] T. Adye,[61] N. De Groot,[61] B. Franek,[61] N. I. Geddes,[61] G. P. Gopal,[61] S. M. Xella,[61] R. Aleksan,[62] S. Emery,[62] A. Gaidot,[62] S. F. Ganzhur,[62] P.-F. Giraud,[62] G. Hamel de Monchenault,[62] W. Kozanecki,[62] M. Langer,[62] G. W. London,[62] B. Mayer,[62] B. Serfass,[62] G. Vasseur,[62] Ch. Yèche,[62] M. Zito,[62] M. V. Purohit,[63] H. Singh,[63] A. W. Weidemann,[63] F. X. Yumiceva,[63] I. Adam,[64] D. Aston,[64] N. Berger,[64] A. M. Boyarski,[64] G. Calderini,[64] M. R. Convery,[64] D. P. Coupal,[64] D. Dong,[64] J. Dorfan,[64] W. Dunwoodie,[64] R. C. Field,[64] T. Glanzman,[64] S. J. Gowdy,[64] T. Haas,[64] V. Halyo,[64] T. Himel,[64] T. Hryn'ova,[64] M. E. Huffer,[64] W. R. Innes,[64] C. P. Jessop,[64] M. H. Kelsey,[64] P. Kim,[64] M. L. Kocian,[64] U. Langenegger,[64] D. W. G. S. Leith,[64] S. Luitz,[64] V. Luth,[64] H. L. Lynch,[64] H. Marsiske,[64] S. Menke,[64] R. Messner,[64] D. R. Muller,[64] C. P. O'Grady,[64] V. E. Ozcan,[64] A. Perazzo,[64] M. Perl,[64] S. Petrak,[64] H. Quinn,[64] B. N. Ratcliff,[64] S. H. Robertson,[64] A. Roodman,[64] A. A. Salnikov,[64] T. Schietinger,[64] R. H. Schindler,[64] J. Schwiening,[64] A. Snyder,[64] A. Soha,[64] S. M. Spanier,[64] J. Stelzer,[64] D. Su,[64] M. K. Sullivan,[64] H. A. Tanaka,[64] J. Va'vra,[64] S. R. Wagner,[64] M. Weaver,[64] A. J. R. Weinstein,[64] W. J. Wisniewski,[64] D. H. Wright,[64] C. C. Young,[64] P. R. Burchat,[65] C. H. Cheng,[65] T. I. Meyer,[65] C. Roat,[65] R. Henderson,[66] W. Bugg,[67] H. Cohn,[67] J. M. Izen,[68] I. Kitayama,[68] X. C. Lou,[68] F. Bianchi,[69] M. Bona,[69] D. Gamba,[69] L. Bosisio,[70] G. Della Ricca,[70] S. Dittongo,[70] L. Lanceri,[70] P. Poropat,[70] G. Vuagnin,[70] R. S. Panvini,[71] C. M. Brown,[72] P. D. Jackson,[72] R. Kowalewski,[72] J. M. Roney,[72] H. R. Band,[73] E. Charles,[73] S. Dasu,[73] M. Datta,[73] A. M. Eichenbaum,[73] H. Hu,[73] J. R. Johnson,[73] R. Liu,[73] F. Di Lodovico,[73] Y. Pan,[73] R. Prepost,[73] I. J. Scott,[73] S. J. Sekula,[73] J. H. von Wimmersperg-Toeller,[73] S. L. Wu,[73] Z. Yu,[73] T. M. B. Kordich,[74] and H. Neal[74]

(The *BABAR* Collaboration)

[1]*Laboratoire de Physique des Particules, F-74941 Annecy-le-Vieux, France*
[2]*Università di Bari, Dipartimento di Fisica and INFN, I-70126 Bari, Italy*
[3]*Institute of High Energy Physics, Beijing 100039, China*
[4]*University of Bergen, Inst. of Physics, N-5007 Bergen, Norway*
[5]*Lawrence Berkeley National Laboratory and University of California, Berkeley, CA 94720, USA*
[6]*University of Birmingham, Birmingham, B15 2TT, United Kingdom*
[7]*Ruhr Universität Bochum, Institut für Experimentalphysik 1, D-44780 Bochum, Germany*
[8]*University of Bristol, Bristol BS8 1TL, United Kingdom*
[9]*University of British Columbia, Vancouver, BC, Canada V6T 1Z1*
[10]*Brunel University, Uxbridge, Middlesex UB8 3PH, United Kingdom*
[11]*Budker Institute of Nuclear Physics, Novosibirsk 630090, Russia*
[12]*University of California at Irvine, Irvine, CA 92697, USA*
[13]*University of California at Los Angeles, Los Angeles, CA 90024, USA*
[14]*University of California at San Diego, La Jolla, CA 92093, USA*
[15]*University of California at Santa Barbara, Santa Barbara, CA 93106, USA*
[16]*University of California at Santa Cruz, Institute for Particle Physics, Santa Cruz, CA 95064, USA*
[17]*California Institute of Technology, Pasadena, CA 91125, USA*
[18]*University of Cincinnati, Cincinnati, OH 45221, USA*
[19]*University of Colorado, Boulder, CO 80309, USA*
[20]*Colorado State University, Fort Collins, CO 80523, USA*
[21]*Technische Universität Dresden, Institut für Kern- und Teilchenphysik, D-01062 Dresden, Germany*
[22]*Ecole Polytechnique, F-91128 Palaiseau, France*
[23]*University of Edinburgh, Edinburgh EH9 3JZ, United Kingdom*
[24]*Elon University, Elon University, NC 27244-2010, USA*
[25]*Università di Ferrara, Dipartimento di Fisica and INFN, I-44100 Ferrara, Italy*
[26]*Florida A&M University, Tallahassee, FL 32307, USA*

^{27}Laboratori Nazionali di Frascati dell'INFN, I-00044 Frascati, Italy
^{28}Università di Genova, Dipartimento di Fisica and INFN, I-16146 Genova, Italy
^{29}Harvard University, Cambridge, MA 02138, USA
^{30}University of Iowa, Iowa City, IA 52242, USA
^{31}Iowa State University, Ames, IA 50011-3160, USA
^{32}Laboratoire de l'Accélérateur Linéaire, F-91898 Orsay, France
^{33}Lawrence Livermore National Laboratory, Livermore, CA 94550, USA
^{34}University of Liverpool, Liverpool L69 3BX, United Kingdom
^{35}University of London, Imperial College, London, SW7 2BW, United Kingdom
^{36}Queen Mary, University of London, E1 4NS, United Kingdom
^{37}University of London, Royal Holloway and Bedford New College, Egham, Surrey TW20 0EX, United Kingdom
^{38}University of Louisville, Louisville, KY 40292, USA
^{39}University of Manchester, Manchester M13 9PL, United Kingdom
^{40}University of Maryland, College Park, MD 20742, USA
^{41}University of Massachusetts, Amherst, MA 01003, USA
^{42}Massachusetts Institute of Technology, Laboratory for Nuclear Science, Cambridge, MA 02139, USA
^{43}McGill University, Montréal, QC, Canada H3A 2T8
^{44}Università di Milano, Dipartimento di Fisica and INFN, I-20133 Milano, Italy
^{45}University of Mississippi, University, MS 38677, USA
^{46}Université de Montréal, Laboratoire René J. A. Lévesque, Montréal, QC, Canada H3C 3J7
^{47}Mount Holyoke College, South Hadley, MA 01075, USA
^{48}Università di Napoli Federico II, Dipartimento di Scienze Fisiche and INFN, I-80126, Napoli, Italy
^{49}University of Notre Dame, Notre Dame, IN 46556, USA
^{50}Oak Ridge National Laboratory, Oak Ridge, TN 37831, USA
^{51}University of Oregon, Eugene, OR 97403, USA
^{52}Università di Padova, Dipartimento di Fisica and INFN, I-35131 Padova, Italy
^{53}Universités Paris VI et VII, Lab de Physique Nucléaire H. E., F-75252 Paris, France
^{54}Università di Pavia, Dipartimento di Elettronica and INFN, I-27100 Pavia, Italy
^{55}University of Pennsylvania, Philadelphia, PA 19104, USA
^{56}Università di Pisa, Scuola Normale Superiore and INFN, I-56010 Pisa, Italy
^{57}Prairie View A&M University, Prairie View, TX 77446, USA
^{58}Princeton University, Princeton, NJ 08544, USA
^{59}Università di Roma La Sapienza, Dipartimento di Fisica and INFN, I-00185 Roma, Italy
^{60}Universität Rostock, D-18051 Rostock, Germany
^{61}Rutherford Appleton Laboratory, Chilton, Didcot, Oxon, OX11 0QX, United Kingdom
^{62}DAPNIA, Commissariat à l'Energie Atomique/Saclay, F-91191 Gif-sur-Yvette, France
^{63}University of South Carolina, Columbia, SC 29208, USA
^{64}Stanford Linear Accelerator Center, Stanford, CA 94309, USA
^{65}Stanford University, Stanford, CA 94305-4060, USA
^{66}TRIUMF, Vancouver, BC, Canada V6T 2A3
^{67}University of Tennessee, Knoxville, TN 37996, USA
^{68}University of Texas at Dallas, Richardson, TX 75083, USA
^{69}Università di Torino, Dipartimento di Fisica Sperimentale and INFN, I-10125 Torino, Italy
^{70}Università di Trieste, Dipartimento di Fisica and INFN, I-34127 Trieste, Italy
^{71}Vanderbilt University, Nashville, TN 37235, USA
^{72}University of Victoria, Victoria, BC, Canada V8W 3P6
^{73}University of Wisconsin, Madison, WI 53706, USA
^{74}Yale University, New Haven, CT 06511, USA
(Dated: February 7, 2008)

We report a measurement of the branching fraction of the decay $B^0 \to D^{*+}D^{*-}$ and of the CP-odd component of its final state using the BABAR detector. With data corresponding to an integrated luminosity of $20.4\,\text{fb}^{-1}$ collected at the $\Upsilon(4S)$ resonance during 1999-2000, we have reconstructed 38 candidate signal events in the mode $B^0 \to D^{*+}D^{*-}$ with an estimated background of 6.2 ± 0.5 events. From these events, we determine the branching fraction to be $\mathcal{B}(B^0 \to D^{*+}D^{*-}) = (8.3\pm1.6(stat)\pm 1.2(syst)) \times 10^{-4}$. The measured CP-odd fraction of the final state is $0.22 \pm 0.18(stat) \pm 0.03(syst)$.

PACS numbers: 13.25.Hw, 12.15.Hh, 11.30.Er

After the observation of time-dependent CP-violating asymmetries in the decays of neutral B mesons to CP eigenstates containing charmonium [1, 2], it is interesting to extend the search for CP-violating effects to Cabibbo-suppressed double charm modes, such as $B^0 \to D^{(*)+}D^{(*)-}$ [3]. The interference of the dominant tree amplitude with the mixing diagram is sensitive to the angle β of the Unitarity Triangle in this case as well;

however, the theoretically uncertain contribution of penguin amplitudes with different weak phases is potentially significant and may shift the observed asymmetry by an amount that depends on the ratio of the penguin and tree contributions and their relative weak phases. The $B^0 \to D^{*+}D^{*-}$ vector-vector final state has very clear experimental signatures that make it an interesting candidate for CP-violation measurements. However, it is not a pure CP eigenstate and a dilution of the measured asymmetry can be produced by a P-wave, CP-odd, component. A time-dependent angular analysis of the decay products [4] can remove the dilution by resolving the CP-even and CP-odd components. As a precursor to measuring time-dependent CP-violating asymmetries using the decay $B^0 \to D^{*+}D^{*-}$, we report in this letter a measurement of the $B^0 \to D^{*+}D^{*-}$ branching fraction and a measurement of the CP-odd component, $R_\perp$, of the final state. These measurements represent significant improvements over the previous measurements $\mathcal{B}(B^0 \to D^{*+}D^{*-}) = (9.9^{+4.2}_{-3.3}(stat) \pm 1.2(syst)) \times 10^{-4}$ and $(1 - R_\perp) < 0.11$ at 90% C.L. [5].

The data used in this analysis were collected with the BABAR detector [6] at the PEP-II storage ring [7] located at the Stanford Linear Accelerator Center. This data sample represents an integrated luminosity of $20.4\,\text{fb}^{-1}$ collected on the $\Upsilon(4S)$ resonance. Assuming 50% of the $\Upsilon(4S)$ decays give $B^0\overline{B}^0$, the number of neutral B mesons in this sample is $(22.8 \pm 0.4) \times 10^6$.

Charged particles are detected and their momenta measured with the combination of a 40-layer drift chamber (DCH) and a five-layer silicon vertex tracker (SVT), both operating in a 1.5 T solenoidal magnetic field. The charged particle tracking system allows particles with low momentum in the laboratory frame to be reconstructed efficiently, a property that is very important for this analysis. This efficiency begins to turn on at a momentum of $\sim 60\,\text{MeV}/c$ and reaches its maximum value at around $200\,\text{MeV}/c$. Photons are detected by a CsI(Tl) electromagnetic calorimeter (EMC) that provides high detection for energies above 20 MeV, with typical energy and angular resolutions of 3% and 4 mrad, respectively, for 1 GeV photons. Charged particle identification is provided by the ionization loss measurements in the SVT and DCH, and by an internally reflecting ring-imaging Cherenkov detector (DIRC) covering the central region of the detector.

Events are selected by requiring three or more charged tracks and that the normalized second Fox-Wolfram moment [8] of the event be less than 0.6. We also require that the cosine of the angle between the reconstructed B direction and the thrust axis of the rest of the event, calculated in the $\Upsilon(4S)$ rest frame, be less than 0.9. These criteria discriminate $\Upsilon(4S)$ events from non-resonant background events.

B^0 mesons are exclusively reconstructed by combining two charged D^* candidates, using a number of D^{*+} and D decay modes. The D^{*+} mesons are reconstructed in their decays $D^{*+} \to D^0\pi^+$ and $D^{*+} \to D^+\pi^0$. We include in this analysis the decay combinations $D^{*+}D^{*-}$ decaying to $(D^0\pi^+, \overline{D}^0\,\pi^-)$ or $(D^0\pi^+, D^-\pi^0)$, but not $(D^+\pi^0, D^-\pi^0)$ due to the smaller branching fraction and larger expected backgrounds. D^0 and D^+ candidates are subjected to a mass-constrained fit to provide an improved measurement of the D meson's momentum. They are combined with pion candidates, referred to as "soft" pions due to their low $(< 200\,\text{MeV}/c)$ transverse momentum, to form D^{*+} candidates. A topological vertex fit is performed that includes the mean position of the e^+e^- interaction point to improve the angular resolution of the soft pion.

The decay modes of the D^0 and D^+ are selected by an optimization of $S^2/(S+B)$ based on Monte Carlo simulations, where S and B are the expected number of signal and background events, repsectively. We first determine, based on Monte Carlo simulations, the expected $S - B$ for each of the decay mode combinations individually. Then, we successively add modes in order of decreasing $S - B$ to compute an overall $S^2/(S+B)$ value until $S^2/(S+B)$ no longer increases. The decay modes used are $D^0 \to K^-\pi^+$, $D^0 \to K^-\pi^+\pi^0$, $D^0 \to K^-\pi^+\pi^-\pi^+$, $D^0 \to K^0_S\pi^-\pi^+$, $D^+ \to K^-\pi^+\pi^+$, $D^+ \to K^0_S\pi^+$, and $D^+ \to K^-K^+\pi^+$. D^0 (D^+) meson candidates are required to have a reconstructed invariant mass within $20\,\text{MeV}/c^2$ of the nominal D^0 (D^+) mass [9].

Charged kaon candidates are required to be inconsistent with the pion hypothesis, as inferred from the Cherenkov angle measured by the DIRC and the ionizations measured by the SVT and DCH. No particle identification is required for the kaon from the decay $D^0 \to K^-\pi^+$.

$K^0_S \to \pi^+\pi^-$ candidates are required to have an invariant mass within $15\,\text{MeV}/c^2$ of the nominal K^0_S mass. The angle between the flight direction and the momentum vector of the K^0_S candidate is required to be less than 200 mrad, and the transverse flight distance from the primary event vertex, obtained from the remaining charged tracks in the event, must be greater than 2 mm.

Neutral pion candidates are formed from pairs of photons in the EMC with energy above 30 MeV, an invariant mass within $35\,\text{MeV}/c^2$ of the nominal π^0 mass, and a summed energy greater than 200 MeV. A mass-constrained fit is applied to these π^0 candidates. In the case of the soft π^0 from $D^{*+} \to D^+\pi^0$ decays, the energy cut is replaced by a momentum cut, in the $\Upsilon(4S)$ frame, of $70 < p^* < 450\,\text{MeV}/c$.

To select B^0 candidates with well reconstructed D^{*+} and D mesons, we form a χ^2 that includes all measured D^{*+} and D masses:

$$\chi^2_{Mass} = \left(\frac{m_D - \hat{m}_D}{\sigma_{m_D}}\right)^2 + \left(\frac{m_{\overline{D}} - \hat{m}_{\overline{D}}}{\sigma_{m_{\overline{D}}}}\right)^2$$
$$+ \left(\frac{\Delta m_{D^*} - \Delta \hat{m}_{D^*}}{\sigma_{\Delta m_{D^*}}}\right)^2 + \left(\frac{\Delta m_{\overline{D}^*} - \Delta \hat{m}_{\overline{D}^*}}{\sigma_{\Delta m_{\overline{D}^*}}}\right)^2, \quad (1)$$

where the caret over a value refers to the nominal value, and Δm_{D^*} is the $D^{*+} - D$ mass difference. For σ_{m_D} we use values computed for each D candidate, while for $\sigma_{\Delta m_{D^*}}$ we use fixed values of $0.83\,\mathrm{MeV}/c^2$ for $D^{*+} \to D^0\pi^+$ and $1.18\,\mathrm{MeV}/c^2$ for $D^{*+} \to D^+\pi^0$. A requirement that $\chi^2_{Mass} < 20$ is applied to all B^0 candidates. In events with more than one B^0 candidate, we choose the candidate with the lowest value of χ^2_{Mass}.

A B meson candidate is characterized by two kinematic variables: the energy-substituted mass,

$$m_{\mathrm{ES}} \equiv \sqrt{E^{*2}_{Beam} - p^{*\,2}_B}, \quad (2)$$

and the difference of the B candidate's energy from the beam energy,

$$\Delta E \equiv E^*_B - E^*_{Beam}. \quad (3)$$

E^*_B (p^*_B) are the energy (momentum) of the B candidate in the center-of-mass frame and E^*_{Beam} is one-half of the total center-of-mass energy. The signal region in the ΔE vs. m_{ES} plane is defined to be $|\Delta E| < 25\,\mathrm{MeV}$ and $5.273 < m_{\mathrm{ES}} < 5.285\,\mathrm{GeV}/c^2$. Based on Monte Carlo simulations, the width of this region corresponds to approximately $\pm 2.5\sigma$ in both ΔE and m_{ES}.

To determine the expected contribution from background in the signal region, we scale the number of events seen in a sideband in the ΔE vs. m_{ES} plane defined as $|\Delta E| < 200\,\mathrm{MeV}$, $5.20\,\mathrm{GeV}/c^2 < m_{\mathrm{ES}} < 5.26\,\mathrm{GeV}/c^2$ and $50\,\mathrm{MeV} < |\Delta E| < 200\,\mathrm{MeV}$, $5.26 < m_{\mathrm{ES}} < 5.29\,\mathrm{GeV}/c^2$. The scaling factor is calculated by parameterizing the shape of the background in the ΔE vs. m_{ES} plane as the product of an ARGUS function [10] in m_{ES} and a first-order polynomial in ΔE. Based on this parameterization we estimate that the ratio of the number of background events in the signal region to the number of events in the sideband region is $(1.72 \pm 0.10) \times 10^{-2}$. The uncertainty is derived from the observed variation of this ratio under alternative assumptions for the background shape in m_{ES} and ΔE using Monte Carlo simulations. The simulations also indicate that there are no significant sources of background appearing in the signal region beyond that indicated by the sideband extrapolation.

After all selection criteria, 38 events are located in the signal region, with 363 events in the sideband region. The latter, together with the scaling factor determined above, implies an expected number of background events in the signal region of $6.24 \pm 0.33(stat) \pm 0.36(syst)$. The systematic uncertainty comes from the background shape variation mentioned previously. Figure 1 shows a projection of the data on the m_{ES} axis after requiring $|\Delta E| < 25\,\mathrm{MeV}$.
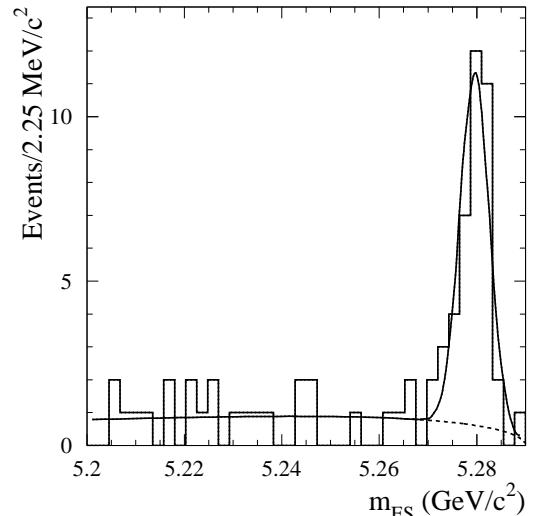

FIG. 1: The m_{ES} istribution of $B^0 \to D^{*+}D^{*-}$ events with $|\Delta E| < 25\,\mathrm{MeV}$. The curve represents a fit with the sum of a Gaussian to model the signal and an ARGUS function [10] to model the background shape.

We use a Monte Carlo simulation of the BABAR detector to determine the efficiency for reconstructing the signal. The efficiencies range from 17.4% to 2.7%, depending on the D decay modes. This, together with the total number of neutral B mesons produced during data collection, allows us to determine the branching fraction for $B^0 \to D^{*+}D^{*-}$ to be

$$\mathcal{B}(B^0 \to D^{*+}D^{*-}) = (8.3 \pm 1.6(stat) \pm 1.2(syst)) \times 10^{-4}.$$

The high charged particle multiplicity makes this measurement particularly sensitive to the tracking system. Therefore the dominant systematic uncertainty comes from our level of understanding of the charged particle tracking efficiency. Systematic errors are assigned on a per track basis for π, K, and soft π, and are added linearly (9.9%). The effect on acceptance due to the imprecisely known partial-wave content of the $B^0 \to D^{*+}D^{*-}$ final state is another source of potential systematic bias (6.6%). Other significant potential systematic biases arise due to the uncertainties on the branching fractions [9] of the D^{*+}, D^0, and D^+ (5.6%) and the uncertainties in mass resolutions of reconstructed mesons (4.1%). The total systematic uncertainty from all considered sources is 15%.

In addition to the branching fraction quoted above, we have also measured the CP-odd fraction of the final state. This fraction, $R_\perp$, is determined from the angular distribution of the soft pions in the decay, analyzed in the transversity basis [4]. In this reference frame, three decay amplitudes determine the distribution of three decay angles. Integrating over time, B flavor, and two of

these three angles yields the following expression:

$$\frac{1}{\Gamma}\frac{d\Gamma}{d\cos\theta_{\rm tr}} = \frac{3}{4}(1 - R_\perp)\sin^2\theta_{tr} + \frac{3}{2}R_\perp\cos^2\theta_{tr}. \quad (4)$$

Here Γ is the decay rate and θ_{tr} is the angle between the normal to the D^{*-} decay plane and the line of flight of the soft pion from the D^{*+} evaluated in the D^{*+} rest frame.

We perform an unbinned maximum likelihood (ML) fit to the 38 events in the signal region described previously. The fit takes into account the presence of background, whose properties are derived from the sideband sample, and the angular resolution σ_θ estimated from Monte Carlo simulations. We define the likelihood function to be

$$\mathcal{L} = \prod_{i=1,n} \mathcal{L}_i = \prod_{i=1,n} \Big[p \times \mathcal{F}(\theta_{tr,i}, \sigma_{\theta,i}, R_\perp^{sig}) + \\ (1-p) \times \mathcal{F}(\theta_{tr,i}, \sigma_{\theta,i}, R_\perp^{bkg}) \Big], \quad (5)$$

where n is the number of selected events. The contribution to the total likelihood from the i-th event, $\mathcal{L}_i$, is defined in terms of the purity, p, of the sample and the probability density functions $\mathcal{F}(\theta_{tr,i}, \sigma_{\theta,i}, R_\perp)$ for the signal and background. $R_\perp^{sig}$ and $R_\perp^{bkg}$ are the parameters describing the shapes of the signal and background angular distributions, respectively, and $\theta_{tr,i}$ is the measured transversity angle in event i. The probability density functions $\mathcal{F}$ are obtained from the convolution of the angular distribution (Eq. 4) with Gaussian resolution functions describing the measurement uncertainties $\sigma_{\theta,i}$. From studies of simulated data, σ_θ was measured to be 0.11 (0.12) radians for charged (neutral) slow pions. A 10% uncertainty on these values is considered when estimating the corresponding systematic error.

The value of $R_\perp^{bkg}$ is evaluated by fitting the 363 events in the sideband region and setting $p = 0$ in Eq. 5. The result of this fit is $R_\perp^{bkg} = 0.29 \pm 0.04$, compatible with the value expected for a uniform distribution ($R_\perp = 1/3$). To determine $R_\perp^{sig}$, we fit the 38 events in the signal region with $R_\perp^{bkg}$ fixed to 0.29 and p fixed at 83.6%. The result of the fit to the signal region, without the correction for angular acceptance bias described below, is $R_\perp^{sig} = 0.25 \pm 0.18(stat)$, and is shown in Fig. 2. The probability of obtaining a lower likelihood, evaluated using a Monte Carlo technique, is 66%.

It should be noted that Eq. 4 is the differential decay rate Γ integrated over the full ranges of the other two decay angles in the transversity basis, neglecting any bias in the projected θ_{tr} distribution introduced by detector acceptance effects. A detailed study of the kinematics of the decay shows that the incomplete detector coverage of the polar angle with respect to the beam axis does not introduce any bias in the distributions of the decay angles in the transversity basis. However, an inefficiency in detecting soft pions below a threshold in transverse momentum
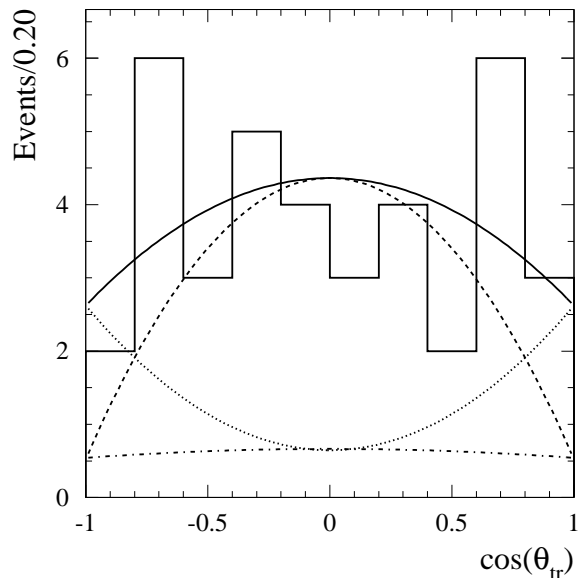

FIG. 2: The $\cos\theta_{tr}$ distribution from the unbinned ML fit, superimposed on the histogram of the $B^0 \to D^{*+}D^{*-}$ candidates in the signal region. The solid line represents the $\cos\theta_{tr}$ distribution from the unbinned ML fit for the selected events. The dotted and dashed lines represent the fitted CP-odd and CP-even components, respectively, for the signal. The dot-dashed curve represents the fitted background component.

may indeed introduce such a bias due to the correlations between the decay angles and particle momenta in the laboratory frame. The amount of these acceptance losses depends on the population of phase space, determined by the values of the decay amplitudes.

An accurate correction for these acceptance effects requires the complete determination of the decay amplitudes using a full angular analysis on a sufficiently large data sample. To estimate the size of the acceptance bias on $R_\perp$ without knowing the decay amplitudes, the fit procedure was tested on several samples of $B^0 \to D^{*+}D^{*-}$ simulated events generated with different sets of decay amplitudes. The different amplitudes affect to varying extents the correlated soft pions' transverse momenta and angular distributions. The fitted $R_\perp$ values were found to be consistent with the generated values in the limit of negligible soft pion inefficiency. Depending on the mix of decay amplitudes, they did reveal a bias once the pion-detection threshold was taken into account. Considering the full possible range of decay amplitudes, the calculated bias on $R_\perp$ ranged from -0.048 to $+0.004$. The central value of this interval is taken as a correction to the fitted $R_\perp^{sig}$, while its half width is taken as an estimate of the corresponding systematic uncertainty (0.026). Additional, smaller systematic uncertainties affecting the $R_\perp$ measurement arise from the imperfect knowledge of the resolution in the transversity angle θ_{tr} (0.006), the angular distribution of the background (0.008), and the purity

of the signal sample (0.0003). The total systematic uncertainty on $R_\perp$ is determined to be 0.028, giving the final corrected result:

$$R_\perp = 0.22 \pm 0.18(stat) \pm 0.03(syst).$$

In summary, we have observed a signal of $31.8 \pm 6.2(stat) \pm 0.4(syst)$ events in the decay $B^0 \to D^{*+}D^{*-}$. Our measurement of the branching ratio is

$$\mathcal{B}(B^0 \to D^{*+}D^{*-}) = (8.3 \pm 1.6(stat) \pm 1.2(syst)) \times 10^{-4}.$$

From the transversity angular distribution of these events, we have also measured the CP-odd fraction, $R_\perp$, of the final state. These measurements provide a starting point for measuring time-dependent CP-violating asymmetries in these decays when more data become available.

[*] Also with Università di Perugia, Perugia, Italy

[†] Also with Università della Basilicata, Potenza, Italy

[1] BABAR Collaboration, B. Aubert et al., Phys. Rev. Lett. **87**, 091801 (2001).

[2] Belle Collaboration, K. Abe et al., Phys. Rev. Lett. **87**, 091802 (2001).

[3] Charge-conjugate states are implied throughout this paper and the symbol $D^{(*)}$ refers to either D or D^*.

[4] I. Dunietz et al., Phys. Rev. D **43**, 2193 (1991).

[5] CLEO Collaboration, E. Lipeles et al., Phys. Rev. D **62**, 032005 (2000).

[6] BABAR Collaboration, B. Aubert et al., "The BABAR Detector," hep-ex/0105044 (2001), to appear in Nucl. Instr. and Meth.

[7] PEP-II Conceptual Design Report, SLAC-R-418 (1993).

[8] G. C. Fox and S. Wolfram, Phys. Rev. Lett. **41**, 1581 (1978).

[9] Particle Data Group, D. E. Groom et al., Eur. Phys. Jour. C **15**, 1 (2000).

[10] ARGUS Collaboration, H. Albrecht et al., Z. Phys. C **48**, 543 (1990).